

# pH-Mediated Catch and Release of Charged Molecules with Porous Hollow Nanocapsules

Sergey A. Dergunov, Jeffrey Durbin, Sambit Pattanaik, and Eugene Pinkhassik\*

Department of Chemistry, Saint Louis University, 3501 Laclede Avenue, St. Louis, Missouri 63103, United States

**S** Supporting Information

**ABSTRACT:** Here, we show that the charge of the nanopores in the nanometer-thin shells of hollow porous nanocapsules can regulate the transport of charged molecules. By changing the pH of external aqueous solution, we can entrap charged molecules in nanocapsules and trigger the release of encapsulated content.

Selectively triggered uptake and release of molecules is useful for creating delivery devices for drugs and imaging agents.<sup>1</sup> pH-mediated catch and release is particularly attractive because it can take advantage of physiological gradients of pH. For example, the pH values are 7.35–7.45 in the bloodstream, 5.4–6.2 in endosomes, and 4.8 in lysosomes, while extracellular pH in the tumors, inflamed tissue, or tissue at early stages of wound healing may range from 5.5 to 6.9.<sup>2</sup>

Previously, pH-regulated uptake and release of molecules was reported for layer-by-layer microcapsules.<sup>3</sup> These polymer capsules expanded and contracted in response to varying pH; as a result, the gaps between polymer chains increased when the capsules were expanded, allowing molecules to pass through. In contracted form, nanocapsules retained entrapped molecules. Other examples include pH-sensitive hydrogels that release content at low pH.<sup>4</sup> Bakajin et al.<sup>5</sup> and Hummer et al.<sup>6</sup> showed pH-regulated transport of ions and small molecules through membranes made of carbon nanotubes.

We and others reported the synthesis of vesicle-templated hollow polymer nanocapsules.<sup>7</sup> Imprinted pores can control the size-selective permeability and permit ultrafast transport of species smaller than the pore size.<sup>7a,b,8</sup>

Porous shells of vesicle-templated nanocapsules are much thinner than biological membranes and are among the thinnest known materials, approaching graphene in thickness. To date, there were no reports that electrostatic repulsion could successfully prevent transport of ions through such membranes. The ability to regulate the transport through nanometer-thin membranes may have profound implications for the design of nanoscale functional devices.

Carboxylic groups are particularly suitable for controlling the charge in the physiological pH range. Typical  $pK_a$  values (4.8 for acetic acid; 4.2 for benzoic acid) suggest that >99% of carboxylic groups will be deprotonated at pH of blood (pH ~7.4), while roughly half of carboxylic groups will be deprotonated at pH of lysosomes (pH ~4.8). To test the hypothesis that the charge of nanopores can regulate the transport, we designed capsules containing carboxylic groups in the pore orifice (Figure 1). We hypothesized that in acidic pH,

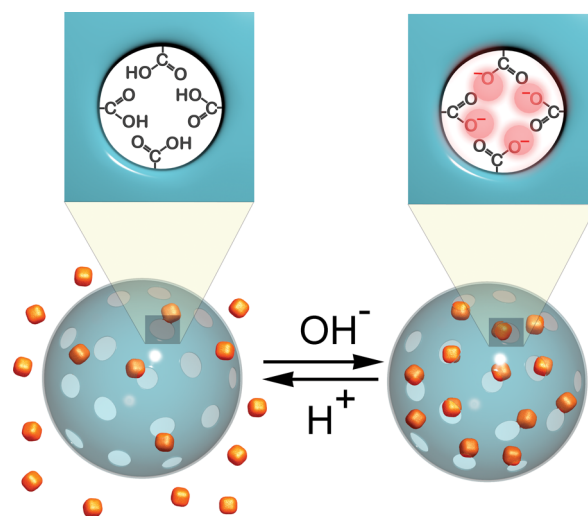


**Figure 1.** Catch and release of small charged molecules in porous hollow nanocapsules: molecules are smaller than the pore size and can diffuse into the capsule at acidic pH but are retained inside the cavity by electrostatic repulsion with negatively charged pores at neutral or basic pH.

neutral pores would permit diffusion of molecules in and out of capsules. In neutral pH, negatively charged pores would not release anions due to electrostatic repulsion.

This pH-mediated catch and release mechanism will permit entrapping molecules in mildly acidic conditions, keeping them entrapped under neutral or basic conditions, and releasing them again in acidic media. The gated transport would not involve rearrangement of the polymer shell or change the size of the nanocapsules. Pores can be imprinted in bilayer-templated membranes with high precision,<sup>7a,b,f,8</sup> and this approach may offer excellent permeability control.

To implement this idea, we synthesized polymer capsules containing multiple carboxylic groups in the pore orifice. Carboxylic groups were imprinted using polymerizable pore-forming templates containing multiple ester groups. The synthesis of nanocapsules is described in detail below.

We designed a simple color scheme to observe the uptake and release of charged molecules. Nanocapsules contain an entrapped large blue molecule that serves a dual purpose. It acts as a size probe showing that the nanopores do not exceed its size in charged or neutral forms and provides a visual contrast

**Received:** October 19, 2013

**Published:** December 25, 2013

for a small yellow molecule during catch and release experiments. We used Reactive Blue dye coupled with  $\beta$ -cyclodextrin (RBCD, Figure 2a) as a blue probe (smallest

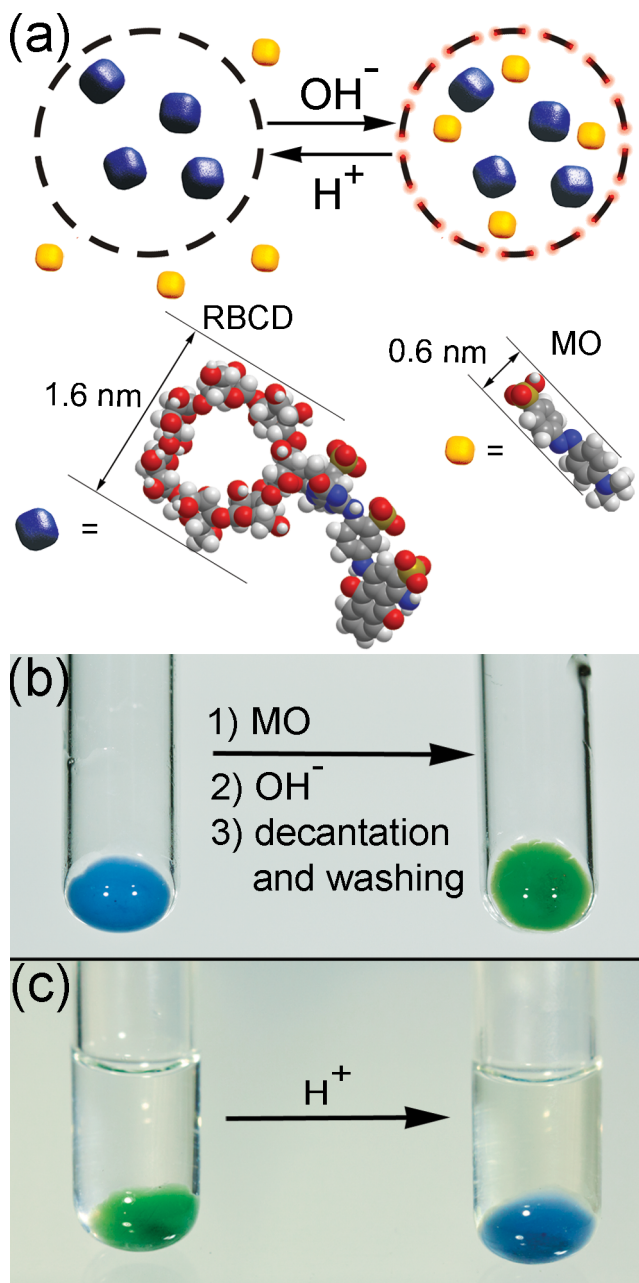


**Figure 2.** pH-regulated uptake and release of small charged molecules in porous hollow nanocapsules. (a) Size probes: blue: Reactive Blue 2/ $\beta$ -cyclodextrin conjugate (RBCD, 1.6 nm);<sup>7b,10</sup> yellow: methyl orange (MO, 0.6 nm). RBCD remains entrapped in nanocapsules. In acidic conditions, electroneutral pores allow MO diffuse in and out of nanocapsules. In neutral and basic media, negatively charged nanopores keep negatively charged MO inside nanocapsules via electrostatic repulsion. (b) Precipitated nanocapsules with entrapped RBCD are treated with an acidic solution of MO, followed by increase in pH and precipitation of nanocapsules. Removal of non-entrapped MO by decantation and washing yields green nanocapsules, showing that both RBCD and MO are now entrapped. (c) Addition of acid to the basic suspension of green nanocapsules with co-entrapped RBCD and MO causes the release of MO, resulting in blue nanocapsules containing RBCD and slightly yellow supernatant.

cross-section 1.6 nm)<sup>7b,10</sup> and methyl orange (MO) as a small anionic yellow dye (smallest cross-section 0.6 nm). The sulfonic group in MO is negatively charged at both neutral and mildly acidic pH. In our approach, capsules are blue when they do not have pinhole defects and retain RBCD (Figure 2). In acidic pH, carboxylic groups in the pore orifice are protonated and the pores are electroneutral. Small anionic MO diffuses into the nanocapsules, and capsules turn green. When the pH is increased to neutral or slightly basic levels, carboxylic groups in the pores become deprotonated and negatively charged. Due to the electrostatic repulsion, anionic molecules cannot escape from the capsules. This color scheme shows immediately whether small yellow molecules are entrapped and retained in nanocapsules. Lowering the pH protonates the carboxylic groups. Following the concentration gradient, anionic molecules can now escape from the nanocapsules, and capsules regain their original blue color.

Nanocapsules containing RBCD were precipitated from an aqueous suspension after the synthesis and removal of non-entrapped dyes (left sample in Figure 2b). In the absence of stabilizing surfactants or lipids, nanocapsules in water form aggregates that can be easily dispersed by mild agitation or stirring. A solution of MO at pH 4 was added to the nanocapsules, the mixture was agitated to allow molecules to enter the capsules, and then the pH was adjusted to 8 with NaOH. Nanocapsules were precipitated and washed in a buffer with mildly basic pH without loss of entrapped MO as evidenced by green color of nanocapsules (right sample in Figure 2b). In control experiments, capsules shown in Figure 2b (left sample) were treated with an aqueous solution of MO at pH 4, and then the capsules were precipitated and washed with a buffer at the same pH. No retention of MO was observed.

In addition to MO, we conducted similar experiments with Congo Red (CR) and 4-(phenylaza)benzoic acid (4-PABA) with similar results. To quantify the retention, we measured the amount of encapsulated dyes at different pH. We found that at pH >8, 100% of entrapped molecules remained entrapped in the capsules even after extensive washing (Supporting Information (SI), Table S2). The amount of entrapped dyes corresponded to the calculated volume fraction of nanocapsules suggesting that all or nearly all of capsules were loaded with anionic dyes at the concentration of the stock solution. At pH 7, we observed 72–81% retention of MO, while at pH 5.5 we found 24–32% retention of MO. At lower pH, no MO remained inside nanocapsules. These data support the central idea of this work, regulation of permeability using electrostatic repulsion.

To show the pH-mediated release, we acidified the aqueous suspension of nanocapsules containing both MO and RBCD to pH 4. A brief agitation and decantation revealed blue capsules and a slightly yellow supernatant (Figure 2c), suggesting that MO was released. After washing the nanocapsules with mildly acidic buffer, the absorbance spectrum of nanocapsules was identical to the spectrum of nanocapsules before the catch and release experiment.

In further control experiments, we showed that dyes did not adsorb on the surface of vesicle-templated capsules at any pH used in this work (SI, Figures S9 and S10). Also, dyes did not adsorb onto a polymer containing carboxylic groups. We conclude that MO, CR, and 4-PABA were indeed retained inside the hollow nanocapsules by the electrostatic repulsion while the carboxylic groups in the pore orifice were

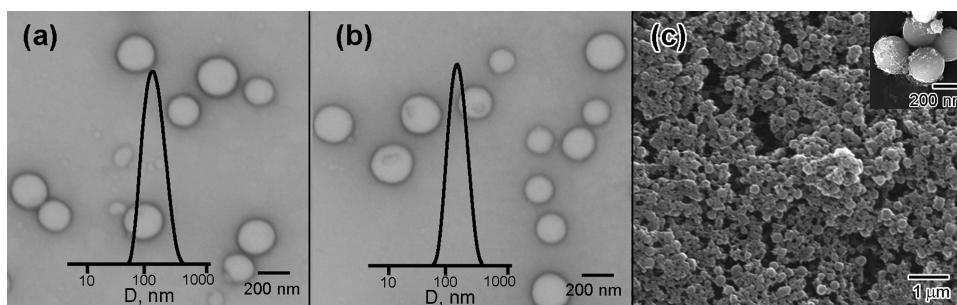


**Figure 3.** Electron micrograph and DLS of nanocapsules. (a,b) TEM images and DLS of polymer nanocapsules at pH 4.3 and 7.1, respectively, corresponding to samples shown in Figure 2b. (c) SEM image of polymer nanocapsules.

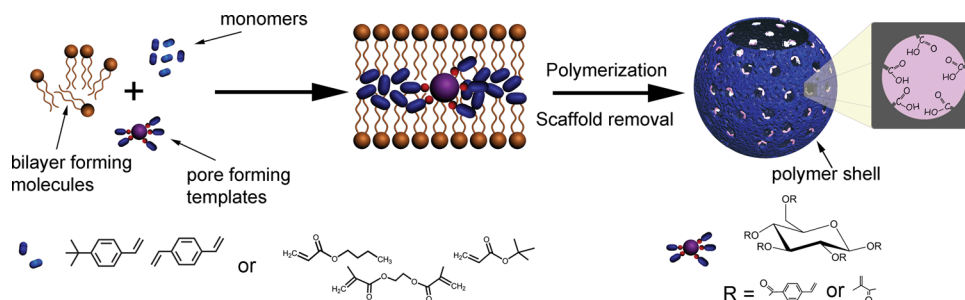


**Figure 4.** Directed assembly of nanometer-thin polymer capsule shells with uniform functionalized nanopores. First step: a self-assembled bilayer is loaded with hydrophobic monomers with cross-linkers and pore-forming template. The template consists of polymerizable moieties (blue) to anchor the template covalently to the polymer matrix, degradable linkers (red) to create a functionalized nanopore, and a bulky hydrophobic unit (violet) to define the pore size. Second step: polymerization produces a cross-linked shell with copolymerized templates in the bilayer interior, followed by the removal of the scaffold and chemical degradation of the template to yield nanometer-thin films containing nanopores decorated with multiple functional groups.

deprotonated. When the carboxylic groups became protonated, the pores permitted transport of charged molecules. Additional experiments with attempted entrapment of glucose and glucosamine, representing a neutral molecule and a cation, respectively, showed no evidence of entrapment (SI, Figures S4–S7). These observations ruled out potential expansion or contraction of pores at different pH and further supported the regulation of transport by electrostatic interactions.

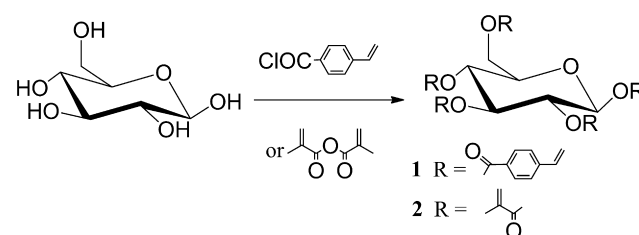
Electron micrographs and data from dynamic light scattering (DLS) analysis demonstrated the preservation of the shape and integrity of the nanocapsules (Figure 3). Transmission electron microscopy (TEM) images and DLS data show that the size and shape of polymer nanocapsules in acidic conditions (Figure 3a) are identical to those in neutral medium (Figure 3b). Average diameter remained 210 nm with polydispersity index values <0.25. Scanning electron microscopy (SEM) images shows clusters of nanocapsules with the same size (Figure 3c). These results suggest that the nanocapsules with nanometer-thin walls are stable at different pH. Exposure of nanocapsules to solutions with different concentrations of small and large osmolytes (up to 2700 mOsm/kg) showed no evidence of rupture of nanocapsules.

Nanocapsules containing imprinted pores with carboxylic groups were synthesized by a directed assembly approach using lipid vesicles (liposomes) as temporary self-assembling scaffolds.<sup>7a–c</sup> Hydrophobic monomers with cross-linkers and pore-forming templates were loaded into the hydrophobic interior of the bilayer (Figure 4). The pore-forming templates were pentaesters of glucose containing polymerizable styrene or methacrylate moieties. These groups copolymerized with monomers and cross-linkers forming a polymer shell inside the bilayer. Following the UV-induced polymerization and

removal of the lipid scaffold, pore-forming templates were hydrolyzed in alkaline medium to form nanopores with carboxylic groups (Figure 4). Previous studies showed that the monomer:cross-linker and monomer:lipid ratios affect the permeability of nanocapsules.<sup>7d,9</sup> In control experiments, we confirmed that the shells of nanocapsules prepared without pore-forming templates were impermeable to the molecules used here (SI, Figure S8 and Table S5).

The pore-forming templates were synthesized by exhaustive esterification of glucose using either *p*-vinylbenzoic acid or methacrylic anhydride (Scheme 1). Typically, glucose and

#### Scheme 1. Synthesis of Polymerizable and Degradable Pore-Forming Templates



esterifying agent were mixed with a base and a catalyst on an ice bath, and the reaction mixture was allowed to warm to room temperature and stirred for 24 h. Synthesis of compound 2 was reported previously.<sup>11</sup>

We used template 1 for the synthesis of polystyrene capsules and template 2 for the synthesis of polyacrylate capsules using monomers and cross-linkers shown in Figure 3.

We used quantitative IR measurements on polystyrene nanocapsules prepared with template **1** to evaluate the average number of carboxylic groups imprinted in each pore. Carboxylic groups on the pore orifice were converted to amide groups by sequential reactions with oxalyl chloride and butylamine. The conversion was done to differentiate the carbonyl groups from the starting ester and resulting amide. The IR absorption band of the carboxylic acid is too close to the absorption band of the ester for confirming that the hydrolysis occurred quantitatively. Also, the intensity of the absorption of the carboxylic group depends on hydrogen bonding, adding uncertainty to quantitative measurements. After the hydrolysis of the pore-forming templates and conversion of the remaining carboxylic groups to the amides, no absorption band for the ester or carboxylic group was found in the IR spectrum (SI, Figure S11). In the IR spectra of capsules before the hydrolysis of the pore-forming templates, the carbonyl band arises from five ester groups per template. After the hydrolysis and conversion of the carboxylic acids to the amides, the carbonyl band appears only due to those carboxylic groups that became part of the polymer shell. Nonreacted vinylbenzoic moieties from the template are removed from the capsules during the hydrolysis. By comparing absorbance of the ester carbonyl in the starting capsules with the absorbance of the amide carbonyl in the functionalized capsules, we found that nanopores in newly prepared nanocapsules contained  $3.3 \pm 0.3$  carboxylic groups on average. This number accounted for the intrinsic molar absorptivity of the ester and amide determined from standard calibration curves. Considering that the synthesis of the capsule shell with embedded templates occurred within the bilayer, essentially, a two-dimensional solvent,<sup>12</sup> incorporation of the majority of the functional groups from the template into the cross-linked shell is a favorable outcome.

In summary, we report a new mechanism for selective uptake and triggered release of charged molecules using porous hollow nanocapsules. The catch and release mechanism is based on electrostatic repulsion and controlling the charge of the nanopores by the pH of the external solution.

It is likely that the release characteristics of nanocapsules can be programmed by varying the number of carboxylic groups per pore and number of pores per capsule. These variations may result in fine-tuning of the pH threshold and/or kinetics of the release of encapsulated cargo. Coupled with previously reported ability to control the size of imprinted pores, this approach can offer a versatile method for controlling the permeability of nanothin porous materials.

Other nanometer-thin materials, such as graphene, may likely control permeability using electrostatic repulsion. These results are likely to have broader implications beyond hollow nanocapsules. Regulating permeability in the nanometer-thin membranes can lead to new functional nanodevices and advanced separation systems.

## ■ ASSOCIATED CONTENT

### 📄 Supporting Information

Detailed experimental procedures and data on uptake and release; synthesis of nanocapsules and pore-forming templates. This material is available free of charge via the Internet at <http://pubs.acs.org>.

## ■ AUTHOR INFORMATION

### Corresponding Author

[epinkhas@slu.edu](mailto:epinkhas@slu.edu)

## Notes

The authors declare no competing financial interest.

## ■ ACKNOWLEDGMENTS

This work was supported by the National Science Foundation (CHE-1316680, CHE-1012951, and CHE-0933363) and Saint Louis University Presidential Research Fund.

## ■ REFERENCES

- (1) (a) Skirtach, A. G.; Muñoz Javier, A.; Kreft, O.; Köhler, K.; Pira Alberola, A.; Möhwald, H.; Parak, W. J.; Sukhorukov, G. B. *Angew. Chem., Int. Ed.* **2006**, *45*, 4612–4617. (b) Tong, W.; Song, X.; Gao, C. *Chem. Soc. Rev.* **2012**, *41*, 6103–6124. (c) Yoshimatsu, K.; Lesel, B. K.; Yonamine, Y.; Beierle, J. M.; Hoshino, Y.; Shea, K. J. *Angew. Chem., Int. Ed.* **2012**, *51*, 2405–2408. (d) Leung, S. J.; Romanowski, M. *Adv. Mater.* **2012**, *24*, 6380–6383. (e) Troutman, T. S.; Leung, S. J.; Romanowski, M. *Adv. Mater.* **2009**, *21*, 2334–2338. (f) Hu, Y.; Litwin, T.; Nagaraja, A. R.; Kwong, B.; Katz, J.; Watson, N.; Irvine, D. J. *Nano Lett.* **2007**, *7*, 3056–3064. (g) Broaders, K. E.; Pastine, S. J.; Grandhe, S.; Fréchet, J. M. J. *Chem. Commun.* **2011**, *47*, 665–667. (h) Beaudette, T. T.; Bachelder, E. M.; Cohen, J. A.; Obermeyer, A. C.; Broaders, K. E.; Fréchet, J. M. J.; Kang, E.-S.; Mende, I.; Tseng, W. W.; Davidson, M. G.; Engleman, E. G. *Mol. Pharmaceutics* **2009**, *6*, 1160–1169.
- (2) (a) Gillies, E. R.; Goodwin, A. P.; Fréchet, J. M. J. *Bioconjugate Chem.* **2004**, *15*, 1254–1263. (b) Mellman, I.; Fuchs, R.; Helenius, A. *Annu. Rev. Biochem.* **1986**, *55*, 663–700.
- (3) Sukhorukov, G. B.; Antipov, A. A.; Voigt, A.; Donath, E.; Möhwald, H. *Macromol. Rapid Commun.* **2001**, *22*, 44–46.
- (4) (a) Renggli, K.; Baumann, P.; Langowska, K.; Onaca, O.; Bruns, N.; Meier, W. *Adv. Funct. Mater.* **2011**, *21*, 1206–1205. (b) Sauer, M.; Streich, D.; Meier, W. *Adv. Mater.* **2001**, *13*, 1649–1651. (c) Duan, Q.; Cao, Y.; Li, Y.; Hu, X.; Xiao, T.; Lin, C.; Pan, Y.; Wang, L. *J. Am. Chem. Soc.* **2013**, *135*, 10542–10549.
- (5) Fornasiero, F.; Park, H. G.; Holt, J. K.; Stadermann, M.; Grigoropoulos, C. P.; Noy, A.; Bakajin, O. *Proc. Natl. Acad. Sci. U.S.A.* **2008**, *105*, 17250–17255.
- (6) (a) Kalra, A.; Garde, S.; Hummer, G. *Proc. Natl. Acad. Sci. U.S.A.* **2003**, *100*, 10175–10180. (b) Yeh, I.-C.; Hummer, G. *Proc. Natl. Acad. Sci. U.S.A.* **2004**, *101*, 12177–12182.
- (7) (a) Dergunov, S. A.; Pinkhassik, E. *Angew. Chem., Int. Ed.* **2008**, *47*, 8264–8267. (b) Danila, D. C.; Banner, L. T.; Karimova, E. J.; Tsurkan, L.; Wang, X. Y.; Pinkhassik, E. *Angew. Chem., Int. Ed.* **2008**, *47*, 7036–7039. (c) Dergunov, S. A.; Kesterson, K.; Li, W.; Wang, Z.; Pinkhassik, E. *Macromolecules* **2010**, *43*, 7785–7792. (d) Gomes, J. F. P. d. S.; Sonnen, A. F. P.; Kronenberger, A.; Fritz, J.; Coelho, M. A. N.; Fournier, D.; Fournier-Nöel, C.; Mauzac, M.; Winterhalter, M. *Langmuir* **2006**, *22*, 7755–7759. (e) Ki, C. D.; Chang, J. Y. *Macromolecules* **2006**, *39*, 3415–3419. (f) Ruyschaert, T.; Germain, M.; Gomes, J. F. P. d. S.; Fournier, D.; Sukhorukov, G. B.; Meier, W.; Winterhalter, M. *IEEE Trans. NanoBiosci.* **2004**, *3*, 49–55.
- (8) (a) Dergunov, S. A.; Pinkhassik, E. *J. Am. Chem. Soc.* **2011**, *133*, 19656–19659. (b) Dergunov, S. A.; Miksa, B.; Ganus, B.; Lindner, E.; Pinkhassik, E. *Chem. Commun.* **2010**, *46*, 1485–1487. (c) Shmakov, S. N.; Dergunov, S. A.; Pinkhassik, E. *Chem. Commun.* **2011**, *47*, 8223–8225.
- (9) (a) Dergunov, S. A.; Schaub, S.; Richter, A. G.; Pinkhassik, E. *Langmuir* **2010**, *26*, 6276–6280. (b) Banner, L. T.; Danila, D. C.; Sharpe, K.; Durkin, M.; Clayton, B.; Anderson, B.; Richter, A. G.; Pinkhassik, E. *Langmuir* **2008**, *24*, 11464–11473.
- (10) Dudman, W. F.; Bishop, C. T. *Can. J. Chem.* **1968**, *46*, 3079–3084.
- (11) Zandanel, C.; Mioskowski, C.; Baati, R.; Wagner, A. *Tetrahedron* **2009**, *65*, 9395–9402.
- (12) (a) Sakamoto, J.; Schlüter, A. D. *Two-Dimensional Polymers in Materials Science and Technology*; Wiley-VCH Verlag GmbH & Co. KGaA: Weinheim, Germany, 2006. (b) Sakamoto, J.; van Heijst, J.; Lukin, O.; Schlüter, A. D. *Angew. Chem., Int. Ed.* **2009**, *48*, 1030–1069.